AIP Applied Physics Letters

Atomic-level quantized reaction of HfOx memristor

Yong-En Syu, Ting-Chang Chang, Jyun-Hao Lou, Tsung-Ming Tsai, Kuan-Chang Chang, Ming-Jinn Tsai, Ying-Lang Wang, Ming Liu, and Simon M. Sze

Citation: Applied Physics Letters **102**, 172903 (2013); doi: 10.1063/1.4802821
View online: http://dx.doi.org/10.1063/1.4802821
View Table of Contents: http://scitation.aip.org/content/aip/journal/apl/102/17?ver=pdfcov
Published by the AIP Publishing

Articles you may be interested in

Improvement of resistive switching uniformity for TiO2-based memristive devices by introducing a thin HfO2 layer
J. Vac. Sci. Technol. B **31**, 06FA04 (2013); 10.1116/1.4831764

Ferroelectric memristor based on Pt/BiFeO3/Nb-doped SrTiO3 heterostructure
Appl. Phys. Lett. **102**, 102901 (2013); 10.1063/1.4795145

In-operando and non-destructive analysis of the resistive switching in the Ti/HfO2/TiN-based system by hard x-ray photoelectron spectroscopy
Appl. Phys. Lett. **101**, 143501 (2012); 10.1063/1.4756897

Conducting nanofilaments formed by oxygen vacancy migration in Ti/TiO2/TiN/MgO memristive device
J. Appl. Phys. **110**, 104511 (2011); 10.1063/1.3662922

Investigation statistics of bipolar multilevel memristive mechanism and characterizations in a thin FeOx transition layer of TiN/SiO2/FeOx/Fe structure
J. Appl. Phys. **110**, 053703 (2011); 10.1063/1.3630119

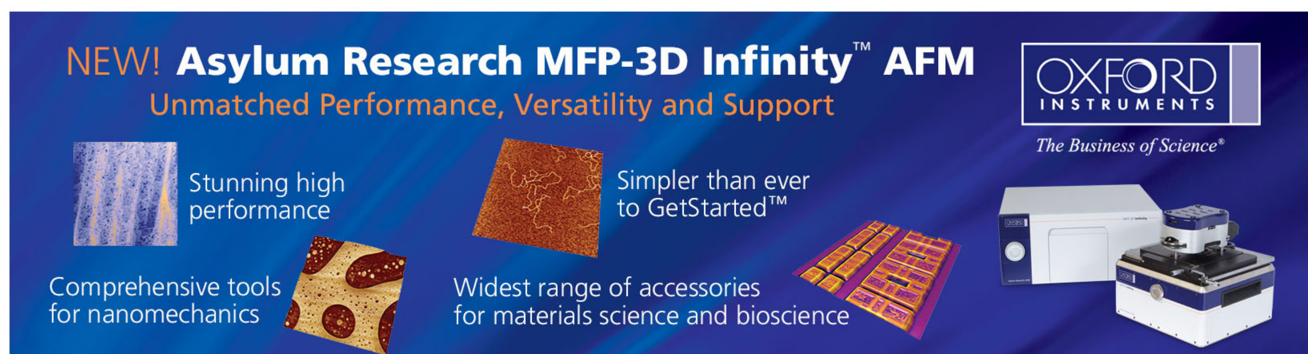

This article is copyrighted as indicated in the article. Reuse of AIP content is subject to the terms at: http://scitation.aip.org/termsconditions. Downloaded to IP: 140.113.38.11 On: Wed, 30 Apr 2014 15:22:21

APPLIED PHYSICS LETTERS **102**, 172903 (2013)

Atomic-level quantized reaction of HfO_x memristor

Yong-En Syu,[1] Ting-Chang Chang,[1,a)] Jyun-Hao Lou,[1] Tsung-Ming Tsai,[2]
Kuan-Chang Chang,[2] Ming-Jinn Tsai,[3] Ying-Lang Wang,[4] Ming Liu,[5] and Simon M. Sze[1,6]
[1]*Department of Physics, National Sun Yat-set University, 70 Lien-hai Road, Kaohsiung 804, Taiwan*
[2]*Department of Materials and Optoelectronic Science, National Sun Yat-Sen University, Kaohsiung 804, Taiwan*
[3]*Electronics and Optoelectronics Research, Industrial Technology Research Institute (ITRI), Hsinchu 300, Taiwan*
[4]*Taiwan Semiconductor Manufacturing Company (TSMC), Tainan 74144, Taiwan*
[5]*Institute of Microelectronics, Chinese Academy of Sciences, Beijing 100029, China*
[6]*Department of Electronics Engineering, National Chiao Tung University, 1001 Ta-Hsueh Road, Hsinchu, Taiwan*

(Received 8 February 2013; accepted 10 April 2013; published online 29 April 2013)

In this study, we have observed dynamic switching behaviors in a memristive device. There are only a few atoms in the resistive switching reaction which enables the high-speed resistive switching characteristics, which was analyzed dynamically by real-time analyzing tools. From fundamental conductance considerations, the resistance of the conductive path in HfO_x memristor is found to be due to barriers which are atomically incremented during the RESET process. Simultaneously, we have demonstrated the quantized switching phenomena at ultra-cryogenic temperature (4 K), which are attributed to the atomic-level reaction in metallic filament. © *2013 AIP Publishing LLC*.
[http://dx.doi.org/10.1063/1.4802821]

An advanced memory technology with high performance, high density, and low power consumption is needed to support the growing needs of mobile devices in the cloud computing era.[1–5] It is required to address the performance gap between logic and storage for future systems on chip. Among emerging memory technologies,[6–12] the memristor has the potential to become the ultimate next-generation nonvolatile memory due to its attributes of simple structure, high speed, and high endurance.[13–22] In particular, the memristor exhibits ultra-high switching speed because the resistive switching behaviors are dominated by variation of several atoms in the device. According to the previous reports, the speed of resistive switching of memristor can be less than 10 ns. The switching speed of memory states of memristor is potentially fast enough to match the operation of CPU.

From the literature, it is understood that the procedure of resistive switching is caused by a sequential redox in memristor.[23–25] The redox mechanism will result in the formation and interrupt of filament, leading to the resistive switching between high resistance state (HRS) and low resistance states (LRS). However, the dimension of the filament is too small to be observed directly by materials analysis tools. Moreover, the atoms involved in the reaction procedure are so few that we need to carefully design an experiment to verify the atomic-level phenomenon in memristor. In general, the atomic-level reaction cannot be examined easily in the room temperature because of the disturbance by electric field and thermal energy in switching material. Therefore, the atomic quantized reactions should be analyzed at the ultra-cryogenic temperature of 4 K.

First, 300 nm wet oxidation was grown on the lightly doped p-type substrate (100) silicon-substrate. SiO_2 layer is used to as an insulator layer between our bottom electrode and silicon substrate to avoid other leakage path from bottom electrode to silicon substrate. Second, a titanium nitride (TiN) bottom electrode 200 nm was deposited by using RF sputter and followed by a SiO_2 deposition. The lithography process was taken to pattern the cell size and active region from 0.24 to 20 μm^2 via. After that, a 5 nm switching layer was grown by using atomic layer deposition (ALD) process. Finally, the 40 nm/10 nm TiN/Ti layer as top electrode and pattern by lithography process. All of the electrical characteristics were measured by the Agilent B1500 semiconductor analyzer. The bias was applied to the bottom electrode (TiN) as the top electrode (Ti) was grounded during the electrical measurement.

The continuous reaction curve of current versus voltage (I-V) in the room temperature can be observed by the black line in Fig. 1. However, a special discontinuous trend of I-V curve was found at 4 K. The ratio of voltage and current possess regularity at some regime of I-V curve. Based on the Ohm's law of $R = V/I$, the different ratios of voltage and current represent different resistance values. The resistance values revealed a regular phenomenon of decreased variation step by step with reset reaction procedure shown in the magnified inset of Fig. 1. The quantized resistive variation can be interpreted as an atomic-level reaction shown in the inset of bottom of Fig. 1.

Figure 2 shows a typical resistance switching characteristics of the $Ti/HfO_2/TiN$ cells which measured in the DC-voltage sweep mode, and exhibited the bipolar behaviors with applied bias on the Ti electrode. For the operation of memristor, an irreversible forming procedure is required to active the as-fabricated memristor cells. A compliance current of 500 μA was set to prevent permanent breakdown during memristor operation in DC-voltage sweeping mode. A sudden increase of the current was observed at the voltage of

a)Email: tcchang@mail.phys.nsysu.edu.tw

 © 2013 AIP Publishing LLC

This article is copyrighted as indicated in the article. Reuse of AIP content is subject to the terms at: http://scitation.aip.org/termsconditions. Downloaded to IP: 140.113.38.11 On: Wed, 30 Apr 2014 15:22:21

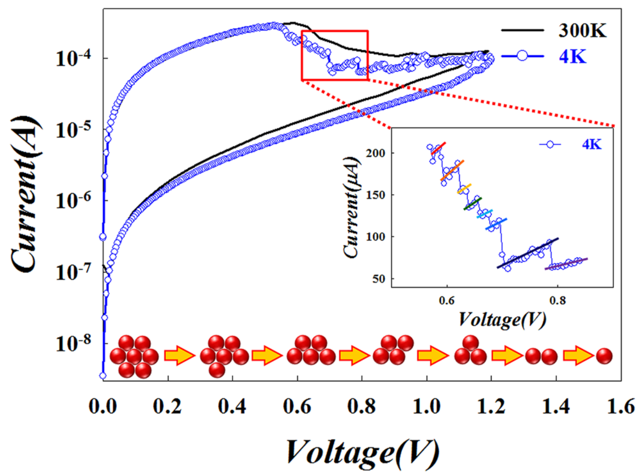

FIG. 1. Quantization reaction for a memristor, compared with continuous reaction. The inset diagram in the bottom part is an illustration to indicate the discontinuous resistance variation due to quantized atomic reaction during reset process.

about 3.5 V to achieve the forming procedure. As the negative bias was swept over the set voltage (V_{set}, −0.55 V), the memristor cell will switch from HRS to LRS, i.e., "set procedure," which is attributed to the formation of filament. The inset diagram in the upper left shows that the set procedure is the transformation of an open circuit situation with HRS changed to a short circuit situation with LRS. Conversely, a gradual descent of current interpreted the cell switched back to HRS from LRS while a positive bias was swept over the reset voltage (V_{reset}, 0.55 V), called as "reset procedure," which is due to the rupture of the filament. The inset diagram in the lower right shows that the reset procedure is the transformation of a low resistance state changed to a higher resistance state. In particular, the reset procedure can be divided into different resistive stages by altering the negative stop voltage of DC sweeping cycle (V_{stop}). The resistance value increases with increasing the V_{stop}, which can be indicated by the stage 1 to stage 5 corresponding to gradually increased V_{stop} (0.7, 0.8, 0.9, 1.0, 1.1 V). We could obtain the multi-level resistance state by controlling the V_{stop}. The variation of resistance state was examined during the reset procedure so as to further comprehend the mechanism of reset reaction in memristor.

In order to ascertain the switching mechanism, the multiple I-V curves in Fig. 2 are fitted to analyze the carrier transport of switching layer. A good linear relationship with a slope of 1 was found in the curve of napierian logarithm leakage current (ln(I)) versus napierian logarithm voltage (ln(V)), indicating that the leakage current in LRS is dominated by Ohmic conduction because the carriers are transported through the continuous filament. The different states of reset I-V curves were fitted and their carrier transport mechanism was analyzed, which represents the multi-high resistance state (multi-HRS) from stage 1 to stage 5 in Fig. 2. The relationship in the curve of ln(I/T^2) versus the square root of the applied voltage ($V^{1/2}$) is linear. This demonstrated that Schottky emission is considered as the main transport mechanism in multi-HRS during the reset procedure. The major leakage current is contributed from the electrons crossing the potential energy barrier between the interface of switching layer and TiN electrode by the thermionic effect. According to the formula of Schottky emission, $J = A^{**}T^2\exp\left[\frac{-q\left(\phi_B-\sqrt{\frac{qV}{4\pi\varepsilon_i d_{sw}}}\right)}{kT}\right]$, where A** is the Richardson constant, the effective switching thickness (d_{sw}) and energy barrier height (ϕ_B) can be obtained from the slope and intercept of the plot of $\sqrt{V}$-ln($\frac{I}{T^2}$), respectively. The slope is $\frac{q}{kT}\sqrt{\frac{q}{4\pi\varepsilon_i d_{sw}}}$ and the intercept is $\ln AA^{**} - \frac{q\phi_B}{kT}$, where the $\varepsilon_i = \kappa\varepsilon_0$, and the κ of HfO_2 is about 25. The $\ln AA^{**}$ can be ignored because it is much smaller than the item of $\frac{q\phi_B}{kT}$. Based on the above-mentioned method, the d_{sw} and ϕ_B of different multi-HRS in Fig. 2 can be obtained through calculation. Figure 3 shows corresponding resistance for different multi-HRS in Fig. 2 with its d_{sw} and ϕ_B. The analytic results exhibit that the ϕ_B were fixed about 0.7 eV and not correlated with corresponding resistance in different multi-HRS, which implicates that the switching layer in different multi-HRS showed similar material properties. However, the d_{sw} was correlated with the resistance value of different multi-HRS. During the reset procedure, the continuous conduction filament will be ruptured gradually leading to

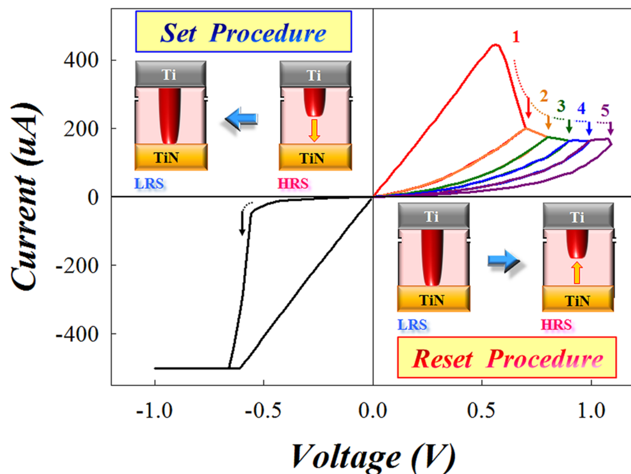

FIG. 2. Memristor operation procedure. The inset in the upper left shows the schematic of the set procedure and the inset in the lower right presents the schematic of the reset procedure.

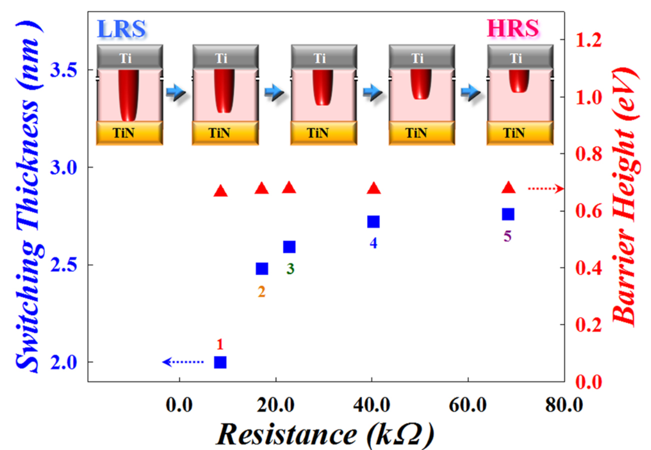

FIG. 3. Different resistance states with effective thickness and energy barrier height. The inset shows the resistance switching procedure which transforms from LRS to HRS, and the distance between filament tip and TiN electrode increases with raising reset voltage.

This article is copyrighted as indicated in the article. Reuse of AIP content is subject to the terms at: http://scitation.aip.org/termsconditions. Downloaded to IP: 140.113.38.11 On: Wed, 30 Apr 2014 15:22:21

the d_{sw} increased, as shown in the insets of upper site of Fig. 3. Therefore, the thickness of switching layer was correlated with the resistance value of different reset multi-HRS, increased with raising V_{stop}.

The above experiment results revealed that the reaction must be begun from the first layer of conductive filament close to the TiN electrode during the reset procedure. During the reaction in the first layer, the effective cross section of contact area will cause the variation of resistance value in memristor. Therefore, we propose a three-dimension diagram of filament in the LRS of memristor to simulate the continuous conduction path connect between the TiN and Ti electrodes as shown in Fig. 4. As oxygen atoms are moved in one after another to recombine the filament, the effective conduction area of filament resulting in decreasing effective conduction area of filament leads to the rise of the resistance value of memristor. The effective area is directly proportional to the numbers of atom connected with the TiN electrode. Therefore, the resistance value is inversely proportional to the number of component atoms of conduction filament, the ratio of resistance with and without i atoms removed away in effective cross section is $R_{N-i}/R_N = N/N-i$. Therefore, the quantized variation of resistance can be obtained due to the atomic-level reaction on the filament during the reset procedure. However, the thermal disturbance effect is so serious, and the reaction speed is so fast that the quantized phenomenon of resistance is hardly to be observed at room temperature. In order to clarify the switching mechanism, the resistance switching characteristics of memristor were measured in the ultra-cryogenic environment to remove the thermodynamic effect during reset procedure. Therefore, the switching resistance transformed step-by-step from low to high resistance states at the temperature of 4 K can be observed in Fig. 1. The phenomena can be speculated that the atoms of effective cross section of conduction path are removed one after another, resulting in the quantized variation on the resistance of memrisor.

The ratio of initial and post-reactive numbers of atom corresponds to a specific ratio of resistance states during the reset procedure. Every transition resistance states can be extracted from the slope of experimental data in Fig. 1 for each quantized step of I-V curve at ultra-cryogenic temperature (4 K). Based on the above-mentioned discussion for resistance calculation, the theoretical resistance ratio of effective cross section between beginning and intermediate states can be calculated according to the removable atoms from the filament. The experimental values complied exactly with the theoretical calculation data as shown in Fig. 5. The results verify that the reaction of reset procedure is an atomic-level reaction, causing conduction area of the effective cross section decreased and the resistance ratio raised. The beginning numbers of atom are 13, which is calculated from the experimental data in the intermediate region of reset procedure as shown in the enlarge inset of Fig. 1. Because the magnitude of change in resistance value is not pronounced at the beginning of reset procedure, the initial variation of atomic numbers was difficult to observe on the effective conduction filament area in initial LRS of memristor. However, we can obtain the atomic numbers of effective cross section in the initial LRS, speculated from the relationship of resistance value and conduction area of filament.

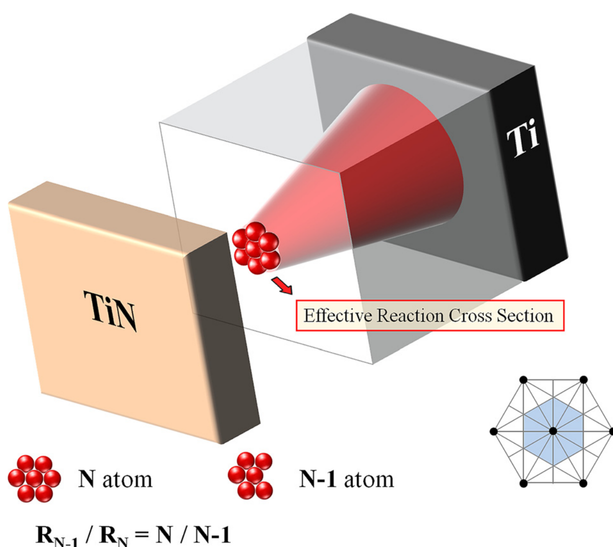

FIG. 4. Filament 3D simulation diagram. The inset at lower right shows the hexagonal-close-packed structure, where the light blue region is the effective cross section area of each atom.

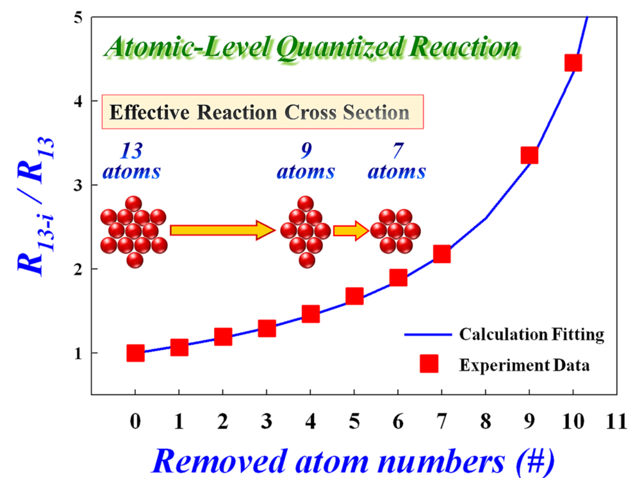

FIG. 5. Atomic-level quantized reaction. The inset shows the numbers of effective cross section atom after reaction.

Because the resistance value of the filament is roughly inversely proportional to the area A and the number of component atoms in the effective cross section is proportional to A, the number of component atoms in the original LRS ($\#_{LRS}$) can be obtained from the resistance of 13 effective atoms ($\#_{13}$) acquired from the experimental data in Fig. 1 as below: $\#_{LRS} = R_{13} \times \#_{13}/R_{LRS} = 2760 \times 13/1920 = 18.68$. If the atoms in the filament are configured with a hexagonal lattice structure, the effective area of each atom can be indicated by the blue region of inset in Fig. 4. While the lattice constant is 0.32 nm, the effective area ($A_{\#}$) of each atom is 0.0887 (nm^2). The effective area (A_{LRS}) of the original LRS can be calculated as $A_{LRS} = \#_{LRS} \times A_{\#} = 18.68 \times 0.0887 = 1.66\,(nm^2)$. According to the simple ohm's law, estimated resistivity, ρ, is 319 ($n\Omega\,m$), which is approximately the theoretical value of Hf metal ($\rho_{Hf} = 331\,(n\Omega\,m)$). Therefore, we consider that the conductive filament for the carrier transport in the LRS is constructed with the elemental Hf.

This article is copyrighted as indicated in the article. Reuse of AIP content is subject to the terms at: http://scitation.aip.org/termsconditions. Downloaded to IP: 140.113.38.11 On: Wed, 30 Apr 2014 15:22:21

In conclusion, the dynamic switching mechanisms during reset procedure in memeristor were completely clarified by a sequential experimental design. A conductive filament composed of oxygen vacancies is confirmed as the initial state of reset reaction procedure. The phenomenon of quantized variation on the resistance of memristor was attributed to the oxygen vacancies change one by one within the effective cross section of conductive filament. Sequentially, the filament near the TiN electrode was oxidized layer by layer, leading to a resistance gradually increase due to the increased barrier layer. We demonstrated that the ultra-fast switching speed of memristor is attributed to several atomic reaction procedures in virtue of the atomic-level quantized phenomena at ultra-cryogenic temperatures.

This work was performed at National Science Council Core Facilities Laboratory for Nano-Science and Nano-Technology in Kaohsiung-Pingtung area and was supported by the National Science Council of the Republic of China under Contract No. NSC 101-2120-M-110-002.

[1]Q. Liu, C. M. Dou, Y. Wang, S. B. Long, W. Wang, M. Liu, M. H. Zhang, and J. N. Chen, Appl. Phys. Lett. **95**, 023501 (2009).
[2]S. W. Tsao, T. C. Chang, S. Y. Huang, M. C. Chen, S. C. Chen, C. T. Tsai, Y. J. Kuo, Y. C. Chen, W. C. Wu, Solid-State Electron. **54**, 1497–1499 (2010).
[3]M. C. Chen, T. C. Chang, S. Y. Huang, K. C. Chang, H. W. Li, S. C. Chen, J. Lu, and Y. Shi, Appl. Phys. Lett. **94**, 162111 (2009).
[4]T. C. Chen, T. C. Chang, T. Y. Hsieh, W. S. Lu, F. Y. Jian, C. T. Tsai, S. Y. Huang, and C. S. Lin, Appl. Phys. Lett. **99**, 022104 (2011).
[5]S. C. Chen, T. C. Chang, P. T. Liu, Y. C. Wu, P. S. Lin, B. H. Tseng, J. H. Shy, S. M. Sze, C. Y. Chang, and C. H. Lien, IEEE Electron Device Lett. **28**, 809–811 (2007).
[6]Y. C. Chen, T. C. Chang, H. W. Li, S. C. Chen, J. Lu, W. F. Chung, Y. H. Tai, and T. Y. Tseng, Appl. Phys. Lett. **96**, 262104 (2010).
[7]C. T. Tsai, T. C. Chang, K. T. Kin, P. T. Liu, P. Y. Yang, C. F. Weng, and F. S. Huang, J. Appl. Phys. **103**, 074108 (2008).
[8]M. Liu, Z. Abid, W. Wang, X. L. He, Q. Liu, and W. H. Guan, Appl. Phys. Lett. **94**, 233106 (2009).
[9]S. Zhang, S. B. Long, W. H. Guan, Q. Liu, Q. Wang, and M. Liu, J. Phys. D: Appl. Phys. **42**, 055112 (2009).
[10]C. T. Tsai, T. C. Chang, P. T. Liu, P. Y. Yang, Y. C. Kuo, K. T. Kin, P. L. Chang, and F. S. Huang, Appl. Phys. Lett. **91**, 012109 (2007).
[11]K. C. Chang, T. M. Tsai, T. C. Chang, Y. E. Syu, C. C. Wang, S. L. Chuang, C. H. Li, D. S. Gan, and S. M. Sze, Appl. Phys. Lett. **99**, 263501 (2011).
[12]T. Y. Tseng and H. Nalwa *Handbook of Nanoceramics and their based Nano Devices* (American Scientific Publishers, USA, 2009), pp. 175–176.
[13]W. H. Guan, S. B. Long, R. Jia, and M. Liu, Appl. Phys. Lett. **91**, 062111 (2007).
[14]Q. Liu, W. H. Guan, S. B. Long, R. Jia, M. Liu, and J. N. Chen, Appl. Phys. Lett. **92**, 012117 (2008).
[15]K. C. Chang, T. M. Tsai, T. C. Chang, Y. E. Syu, S. L. Chuang, C. H. Li, D. S. Gan, S. M. Sze, Electrochem. Solid State Lett. **15**, H65–H68 (2012).
[16]W. H. Guan, M. Liu, S. B. Long, Q. Liu, and W. Wang, Appl. Phys. Lett. **93**, 223506 (2008).
[17]K. C. Chang, T. M. Tsai, T. C. Chang, Y. E. Syu, H. C. Huang, Y. C. Hung, T. F. Young, D. S. Gan, N. J. Ho, Electrochem. Solid State Lett. **14**, K47–K50 (2011).
[18]T. M. Tsai, K. C. Chang, T. C. Chang, Y. E. Syu, K. H. Liao, B. H. Tseng, and S. M. Sze, Appl. Phys. Lett. **101**, 112906 (2012).
[19]Q. Liu, W. H. Guan, S. B. Long, M. Liu, S. Zhang, Q. Wang, and J. N. Chen, J. Appl. Phys. **104**, 114514 (2008).
[20]T. M. Tsai, K. C. Chang, T. C. Chang, G. W. Chang, Y. E. Syu, Y. T. Su, G. R. Liu, K. H. Liao, M. C. Chen, H. C. Huang, Y. H. Tai, D. S. Gan, C. Ye, H. Wang, and S. M. Sze, IEEE Electron Device Lett. **33**, 1693–1695 (2012).
[21]T. M. Tsai, K. C. Chang, T. C. Chang, Y. E. Syu, S. L. Chuang, G. W. Chang, G. R. Liu, M. C. Chen, H. C. Huang, S. K. Liu, Y. H. Tai, D. S. Gan, Y. L. Yang, T. F. Young, B. H. Tseng, K. H. Chen, M. J. Tsai, C. Ye, H. Wang, and S. M. Sze, IEEE Electron Device Lett. **33**, 1696–1698 (2012).
[22]Y. E. Syu, T. C. Chang, T. M. Tsai, G. W. Chang, K. C. Chang, J. H. Lou, Y. H. Tai, M. J. Tsai, Y. L. Wang, and S. M. Sze, IEEE Electron Device Lett. **33**, 342–344 (2012).
[23]T. C. Chang, F. Y. Jian, S. C. Chen, and Y. T. Tsai, Mater. Today **14**, 608–615 (2011).
[24]Y. E. Syu, T. C. Chang, T. M. Tsai, Y. C. Hung, K. C. Chang, M. J. Tsai, M. J. Kao, and S. M. Sze, IEEE Electron Device Lett. **32**, 545–547 (2011).
[25]Y. Wang, Q. Liu, S. B. Long, W. Wang, Q. Wang, M. H. Zhang, S. Zhang, Y. T. Li, Q. Y. Zuo, J. H. Yang, and M. Liu, Nanotechnology **21**, 045202 (2010).

This article is copyrighted as indicated in the article. Reuse of AIP content is subject to the terms at: http://scitation.aip.org/termsconditions. Downloaded to IP: 140.113.38.11 On: Wed, 30 Apr 2014 15:22:21